Viscoelastic response of flow driven by a moving permeable disk

Takahiro Nakashima, Takahisa Shiratori, Yoshihiko Oishi, Yuji Tasaka, Yuichi Murai, Yasushi Takeda, Erich J. Windhab

Graduate School of Engineering, Hokkaido University, N13-W8, Kita-ku, Sapporo, 060-8628, Japan
Swiss Federal Institute of Technology, Zurich, Schmelzbergstrasse 9, 8092 Zurich, Switzerland

nakashima@ring-me.eng.hokudai.ac.jp

Spatiotemporal and time averaged two-dimensional velocity profiles of the flow driven by a moving permeable disk in viscoelastic fluid are measured by Ultrasonic Velocity Profiler (UVP). The motivation of this study is to find a new mixing technique which is utilizing characteristics of viscoelastic flow and also to seek the sources of Flow Induced Vibration (FIV) due to elastic nature. A permeable disk is towed by a moving stage, and flow around the disk is measured by UVP. Two kinds of measurements with different installations of an ultrasonic transducer are examined. First one is Eulerian measurement where the UVP transducer is fixed on the tank. With this setup, we found a velocity fluctuation in the wake behind the permeable disk. Frequency analysis of the data is performed and the cause of the fluctuation is discussed in this paper. Second one is Lagrangian frame measurement where the transducer is towed together with the disk. Comparison of the velocity distributions obtained in flows around the solid and permeable disks indicated how the drag coefficient of the disk changes with porosity and hole diameter of the permeable disk in viscoelastic liquid.

Keywords: Viscoelastic flow, Permeable disk, Polyacrylamide, External flow

1 INTRODUCTION

In polymer processing, mixing has been one of the greatest concerns since viscoelasticity resists local material displacement. Similar issues are struggled in heat transfers and chemical reactions. Generally, sufficiently large power is required to drive viscoelastic fluid, and this worsens the pumping power efficiency in mechanical engineering point of view. The authors seek a method of mixing enhancement by utilizing common properties of target viscoelastic fluids namely, negative wake generation and shear-thinning flow characteristics. These properties are usually known as mixing-resistances, but there is possibility to convert these events to mixing-enhancers by means of a fluid-permeable object as the object for driving fluids. We expect that permeable bodies produce flows in multi-scales and time lags among them and viscoelasticity shows essential differences in flow fields induced by a moving solid body in comparison with ordinal Newtonian fluids.

Doing the present study may also give good knowledge on understanding Flow Induced Vibration (FIV) of viscoelastic external flows. In Newtonian fluid mechanics, FIV has been long investigated [1] [2]. In contrast, FIV in non-Newtonian fluid, particular for viscoelastic fluid has not been comprehensively understood. Such viscoelastic FIV should be carefully considered to avoid system-damaging events in polymer processing, semi-mold material treatment, and biomechanics.

For these two demands in viscoelastic fluid engineering, we carry out experiments on viscoelastic flows driven by moving permeable disks. The experiments consist of factors, a permeable body having many holes and viscoelastic fluid. A permeable body moving in Newtonian fluids produces larger drag than that of solid bodies with the same moving speed. This is because of increased friction in small holes of permeable disks where fluid passes through [3]. In viscoelastic fluids, this trend changes oppositely because of shear-thinning property that allows fluid to go through small holes with less friction. At the same time, viscoelasticity resists recovery of velocity defect in the wake behind permeable body at its far wake region and intensifies the through-flow. Negative wakes, shear-banding and viscoelastic turbulence behind the permeable object can also contribute to the control of flow field.

In this flow configuration, Ultrasound Velocity Profiler (UVP) has been suitably applied for using its advantages, capability for constructing spatiotemporal two-dimensional velocity distributions. Axisymmetric flows are generated by the permeable disk as the macroscopic flow. Hence, an inclined single measurement line of UVP in the setup can capture the global flow. Velocity fluctuations obtained by UVP has broad spectrum has been also validly detected. In this paper, we present the measurement method, measured data, and brief discussion on the results.

2 EXPERIMENTAL CONDITIONS

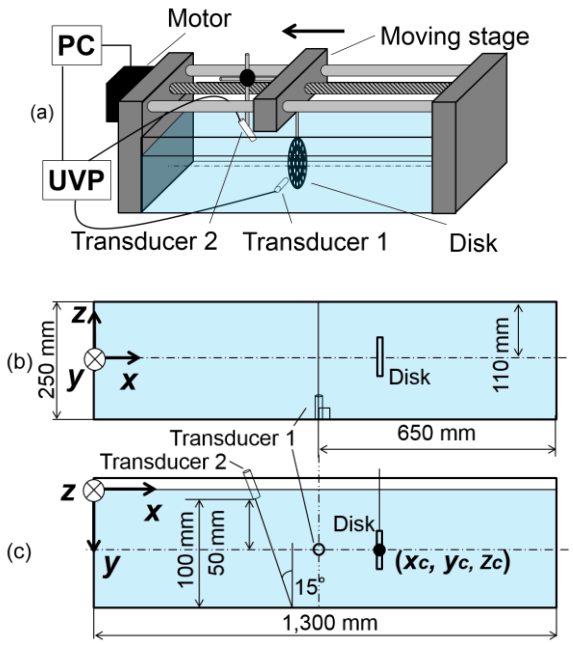

Figure 1: (a) Overall view of experimental setup, (b) top view and (c) side view of experimental setup

Overall view, top view and side view of experimental setup are shown in Fig. 1 (a), (b) and (c), respectively. A moving stage is installed in a tank and a disk is mounted on the moving stage. Towing speed U of moving stage can be controlled by PC and is set at 20 mm/s. The diameter of the disks is 50 mm and the thickness is 2.0 mm. For indicating permeability of the disks, solidity that is the ratio of unholed area to the disk area described in Eq. (1) is used.

$$S = 1 - \frac{nr^2}{R^2}, \tag{1}$$

where R is diameter of the disk, r is holes' diameter and n is the number of holes. In this experiment, two types of disks are used. Their solidities are S = 1.0 (no holes) and S = 0.55 by 4.0 mm diameter holes. As test fluids, two kinds of fluids, tap water and 0.1 wt% polyacrylamide (PAA) solution, are introduced.

In this report, two types of experiments were done with the same experimental setup. First experiment is Eulerian measurement using transducer-1 shown in Fig. 1. Transducer-1 is fixed inside of the tank perpendicular to its lateral wall and its measurement line is horizontal as shown in Fig. 1 (a). The disk is towed from one side to another side of the tank by the moving stage, and passes through in front of transducer 1. Then spatiotemporal velocity profiles of the flow around the moving disk are obtained.

Second experiment is Lagrangian frame measurement using transducer-2. It is fixed on the moving stage and towed together with the disk. Transducer 2 is tilted with 15 degrees to the y axis shown in Fig. 1 (c). The relative position of transducer-2 to the disk can be modified to the x axis direction and this measurement was repeated for some different relative positions. Then, time averaged two-dimensional velocity profiles can be obtained by superposing time-averaged one-dimensional velocity profiles measured at each relative position. The position of the center of the disk is defined as (x_c, y_c, z_c). In both experiments, the basic frequency of transducers is 4.0 MHz.

Here, Reynolds number Re is defined as

$$Re = \frac{UD}{\nu}, \tag{2}$$

where U is towing velocity, D = 50 mm is disk diameter, and ν is kinematic viscosity.

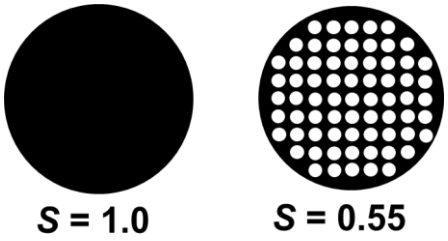

Figure 2: A disk with no holes and a permeable disk

3 RESULTS AND DISCUSSION

3.1 Eulerian measurement

3.1.1 Water

Figure 3 shows the spatiotemporal velocity profile around the permeable disk obtained by Eulerian measurement in the water flow. The disk with S = 0.55 in the solidity is towed. The horizontal and vertical axes mean time and position in the tank from the transducer-1 to the side wall of the tank. The center of the disk is at z - z_c = 50 mm. At t = 0, the UVP measurement is started, and the permeable disk just passes through the front of transducer-1 at about t = 20 sec. Color means z component of velocity. This velocity distribution shows an asymmetric flow field. The setting towing velocity, U = 20 mm/s and corresponding Reynolds number is $Re = 1.0 \times 10^3$. At this Reynolds number, it is known that the wake behind a disk without holes is shedding hairpin vortices periodically [4]. This vortex shedding may break flow symmetry in this flow field.

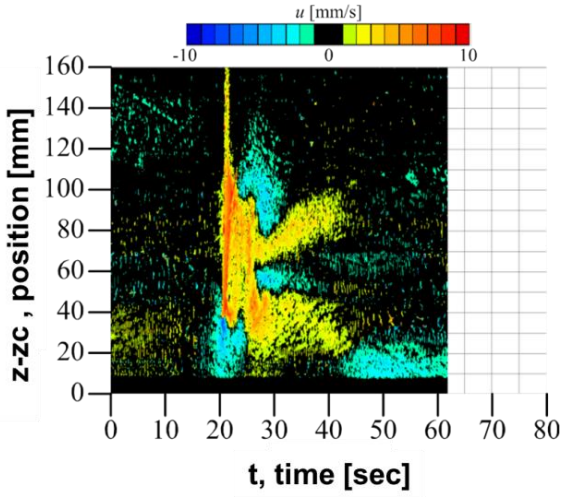

Figure 3: Spatiotemporal velocity profiles around a permeable disk (*S* = 0.55) towed in water

3.1.2 PAA solution 0.1wt%

Spatiotemporal velocity profile obtained in 0.1 wt% PAA solution is shown in Fig. 4. In this case, the disk with *S* = 0.55 passes through the front of the transducer-1 at about *t* = 17 sec. A symmetric flow pattern around this time means a part of the flow avoiding the disk. The most interesting point of Fig. 4 is the wave like stripes behind the disk seen at about *t* = 30 sec. This stripe indicates velocity oscillation. Cause of this oscillation is investigated in the next section.

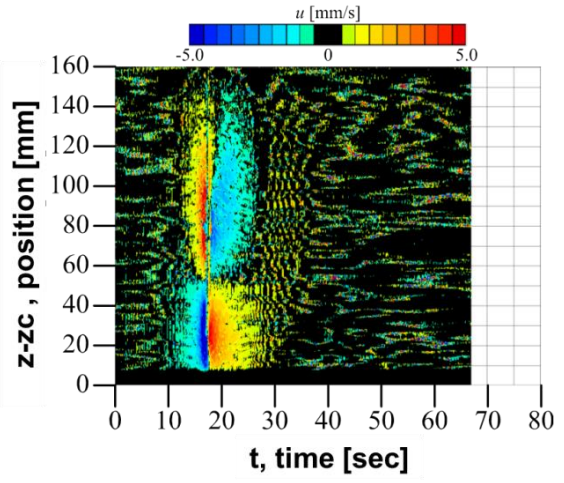

Figure 4: Spatiotemporal velocity profiles around a permeable disk (*S* = 0.55) in PAA solution 0.1wt%

3.1.3 Wavelet transformation

In order to assess this velocity oscillation quantitatively, wavelet transformation [4] is applied to the velocity profile shown in Fig. 4 to the time direction. Gabor mother wavelet is adapted and continuous wavelet transformation is described as follows:

$$WT(b,a) = \frac{1}{\sqrt{|a|}} \int_{-\infty}^{\infty} v(t) \overline{\Psi\left(\frac{t-b}{a}\right)} dt \,, \qquad (3)$$

$$\Psi(t) = \frac{1}{\sqrt{2\pi\sigma^2}} \exp\left(-\frac{t^2}{2\sigma^2}\right) \exp\left(i\omega_0 t\right), \qquad (4)$$

$$p(b,a) = \left|WT(b,a)\right|^2 , \qquad (5)$$

where,

$$\sigma = 1, \varpi_0 = \pi, a = \frac{1}{f\Delta t}\frac{\omega_0}{2\pi} .$$

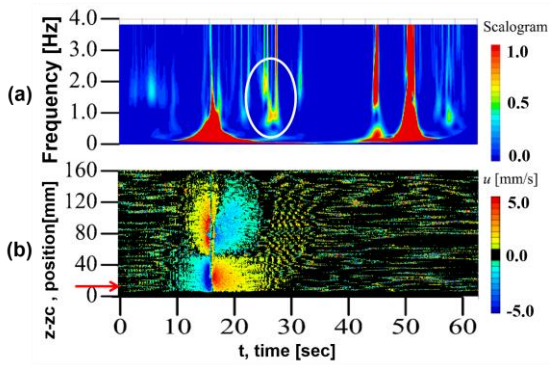

Figure 5: (a) The result of wavelet transformation from (b) spaciotemporal velocity profile

Figure 5 (a) is the result of wavelet transformation. Horizontal axis and vertical axis of the figure mean time and frequency of the velocity fluctuation. Color means power spectral dencity. Figure 5 (b) is a copy of Fig. 4 for comparison, and Fig. 5 (a) and Fig. 5 (b) share the time axis. The wavelet transformation is performed for the velocity variation at z – z0 = 17 mm as indicated by the red arrow in Fig. 5 (b). From the result of wavelet transformation, we can see a peak on the spectorum at the white circled area. This peak corresponds to the velocity oscillation indicated in section 3.1.2. The corresponding frequency *f* is about *f* = 0.5~2.0 Hz.

We expect three candidate factors as the cause of this velocity oscillations: vibration from a motor, inhomogeneity of tracer particles and real flow oscillation. Firstly, the motor is rotating during the experiment to drive the moving stage. When the towing speed of moving stage is 20 mm/s, the rotation speed of motor is around 1.0 Hz. Then, its viblation may be affecting this UVP measurement. Secondly, it is possible that the tracer particles form an inhomogeneous distribution because of elongational flow of the viscoelastic fluid. If once the particles distributes inhomogeneously, the tranceducer will measure velocity properly only when the particle exsists in its measurement volume. Thus the measured velocity profile shows small velocity (properly measured) and extremely large velocity (noise caused by the lack of particles) one

after another. This result in the pattern like a stripe in Fig. 4.

Thirdly, it is possible that viscoelasticity of PAA solution induces oscillatory flow around the disk. Previous researches report unsteady flows named shear wave [6] or viscoelastic instability [1] as characteristic flows of viscoelastic fluid. In viscoelastic flows through a chanel with contraction, periodic vortex shedding occurs [7] because of viscoelasticity. These facts implies that unsteady flows can be induced around the disk. Even in Newtonian fluids, unsteady flows occur around objects as shedding of hair-pin vortices and the corresponding Strouhal number defined as

$$St = \frac{fD}{U}, \qquad (6)$$

takes around 0.16 [5]. In our experiment (f = 0.5 Hz, D = 50 mm and U = 20 mm/s), however, the corresponding Strouhal number is St = 1.25 and is much larger than the hairpin vortex shedding in Newtonian fluid. Thus, we regard the velocity oscillation as specific phenomenon caused by viscoelasticity.

3.2 Lagrangian frame measurement

Time averaged two-dimensional velocity profiles around the disk with S = 1.0 and 0.55 in the solidity are shown in Fig. 6 (a) and (b) as the results of Lagrangian frame measurement, respectively. Color means velocity components of x direction calculated under the assumption of u_y = 0 and u_z = 0. In these graphs, we can see that velocity decreases at x - x_c = 25, y = 50. Large velocity is also measured under the disk, around x - x_c = 0, y = 75. To compare the velocity profiles in Fig. 6 (a) and (b) quantitatively, differences between them are calculated as shown in Fig. 7.

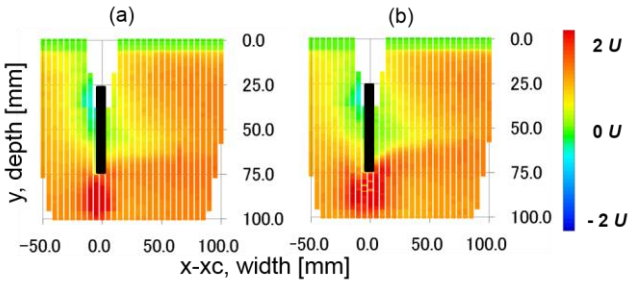

Figure 6: Velocity profiles of 0.1 wt% PAA solution, (a) S = 1.0 and (b) S = 0.55

The velocity profile in Fig. 6 (a) is subtracted from that in Fig. 6 (b). There is an interesting pattern around x - x_c = 25, y = 75. Here, velocity is increased by permeability of the disk. In comparison with the spatiotemporal velocity profile in Eularian frame shown in Fig. 4, this area corresponds to the position where the velocity oscillation occurs. Thus, we can expect that there are both effects of the disk permeability and PAA viscoelasticity.

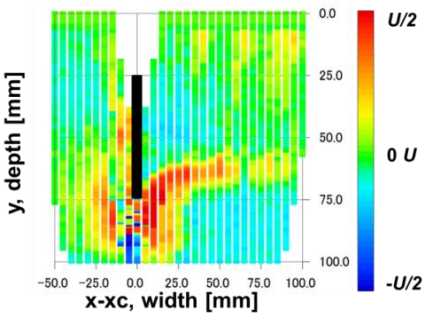

Figure 7: Difference of two velocity profiles of a permeable disk and a disk with no holes

4 CONCLUSION

In order to investigate combination of viscoelasticity and permeability of a permeable disk, spatiotemporal velocity profiles and time averaged two-dimensional velocity profiles around a permeable disk were obtained by two types of experiment; Eularian measurement and Lagrangian frame measurement. Two kinds of disks, a permeable disk and a disk without holes, were towed in tap water and 0.1wt% PAA solution.

In the results of these two experiments, a velocity oscillation at the wake behind the permeable disk was observed. In the same position, there was a large velocity difference between the case of a permeable disk and a disk without holes.

Therefore, it is concluded that the effect of permeability of the disk and viscoelasticity of PAA solution may make a combined effect as velocity oscillation at the wake behind a permeable disk. If this oscillation can be controlled, these results are applied to mixing method for polymer processing and research for the cause of viscoelastic FIV.

As next steps, wavelet transformation in spatial direction should be applied because it is expected that the holes on the disk make velocity profile with spatial periodicity. If the periodicity is accessed quantitatively, we can conclude that effect of permeability on the flow and that of viscoelasticity generates frequent velocity distribution not only on temporal axis but also on spatial axis. Additionally, for verification of whether the velocity oscillation found in Fig. 4 results from viscoelastic instability or not, visualization experiment is also required. By Particle Image Velocimetry (PIV), we will be able to investigate the adequacy of this UVP measurement and vector field of the area where the velocity oscillation is occurring in Fig. 4.

REFERENCES

[1] Larson R.G.: Instabilities in viscoelastic flows, Rheologica Acta 31 (1992), 213-263.

[2] Lam Y.C. et.al: Micromixer based on viscoelastic flow